



## A predictability analysis of network traffic

Aimin Sang\*, San-qi Li

Department of Electrical and Computer Engineering, University of Texas at Austin, Engineering Science Building (ENS) 516, Austin, TX 78712-1084, USA

Received 3 November 2001; accepted 12 November 2001

### Abstract

This paper assesses the predictability of network traffic by considering two metrics: (1) how far into the future a traffic rate process can be predicted with bounded error; (2) what the minimum prediction error is over a specified prediction time interval. The assessment is based on two stationary traffic models: the auto-regressive moving average and the Markov-modulated poisson process. In this paper, we do not aim to propose the best traffic (prediction) model, which is obviously a hard and arguable issue. Instead, we focus on the constrained predictability estimation with assumption and discussion about the modeling accuracy. The specific time scale or bandwidth utilization target of a predictive network control actually forms the constraint. We argue that the two models, though both short-range dependent, can capture statistics of (self-similar) traffic quite accurately for the limited time scales of interests in measurement-based traffic management. This argument, in mathematical terms, simply reflects the fact that the summarized exponential (correlation) functions may approximate a hyperbolic one very well.

Our study reveals that the applicability of traffic prediction is limited by the deteriorating prediction accuracy with increasing prediction interval. From both analytical and numerical studies, we explore the different roles of traffic statistics, either at the 1st-order or the 2nd-order, in traffic predictability. Particularly, the statistical multiplexing and proper measurement (e.g. sampling/filtering) of traffic show positive effects. Experimental results suggest promising backbone traffic prediction, and generally enhanced predictability if small time-scale traffic variations, which are usually of less importance to bandwidth allocation and call admission control, have been filtered out. The numerical results in the paper provide quantized reference to the optimal online traffic predictability for network control purposes. © 2002 Published by Elsevier Science B.V.

*Keywords:* Prediction; Time-scale; ARMA; MMPP; Self-similarity

### 1. Introduction

One of the key issues in measurement-based network control is to predict the bandwidth re-

quirement in the next control time interval based on the online measurement of traffic characteristics. The goal of traffic prediction is to forecast future traffic rate variations as precisely as possible, based on the measured history. Traffic predictability denotes the possibility for prediction to satisfy some precision requirement over desired prediction/control time interval. On one hand, a large prediction interval is needed to provide suf-

\* Corresponding author. Tel.: +1-972-461-6272; fax: +1-972-461-7506.

E-mail addresses: asang@santera.com, sang@ece.utexas.edu (A. Sang), sanqi@ece.utexas.edu (S.-q. Li).

39 ficient time for control actions, and to offset the  
40 inevitable delays caused by traffic measurement  
41 (e.g. sampling/filtering) and traffic prediction  
42 (modeling/computing). On the other hand, a small  
43 prediction error is desirable for the following reason:  
44 control actions based on erroneous prediction  
45 may inadvertently compromise the control performance.  
46 To overcome this problem, one has to be conservative  
47 and set aside network resources, specifically the  
48 bandwidth resource in this paper. Thus, in order to  
49 achieve high resource utilization, a network controller  
50 would prefer precise prediction. Unfortunately, prediction  
51 accuracy deteriorates quickly as the prediction interval  
52 increases. Clearly there is a tradeoff between a large  
53 prediction interval and a small prediction error, which  
54 reflects the tradeoff between the control time interval  
55 and the network efficiency.

57 Furthermore, traffic of different types have their  
58 own inherent nature of predictability. Thus it is  
59 important to characterize the dominating traffic  
60 statistics in the prediction. The same traffic may  
61 show different predictability if looked at different  
62 time-scales, i.e. if its rate process is sampled/  
63 filtered with different time interval. Therefore, it is  
64 critical to understand the measurement impact on  
65 predictability and always tie them together. Consequently  
66 our major concerns can be summarized into the following  
67 questions:

- 68 1. How far into the future can network traffic be  
69 predicted with confidence requirement? In other  
70 words, what is the maximum prediction interval  
71 (MPI) under certain error constraint?
- 72 2. How much network resource has to be reserved  
73 to absorb the prediction uncertainty, if the prediction  
74 interval is specified as the network control time  
75 interval?
- 76 3. What traffic properties, statistically obtained  
77 from traffic measurements, characterize its inherent  
78 predictability? In addition, how do traffic  
79 multiplexing and traffic sampling affect the  
80 predictability estimation?

81 This paper examines all of the above issues.  
82 Ideally, if one knows the future traffic changes, a  
83 congestion-free network control could be simplified  
84 as a dynamic bandwidth allocation according

to the prediction results. If the predicted rate exceeds  
85 the available bandwidth, either additional  
86 bandwidth is needed, or various control mechanisms  
87 must be evoked to re-route existing flows, to  
88 reduce their source rate by negotiation, or to block  
89 new call arrivals. The control time interval  
90 strongly depends on individual control mechanism.  
91 Generally speaking, it is relatively small for  
92 nodal congestion control or dynamic bandwidth  
93 allocation, reasonably large for local call admission  
94 control (CAC) and substantially larger for  
95 (re-)routing. The larger it is, the more the prediction  
96 error has to be tolerated through bandwidth  
97 over-subscription or reinforced control scheme.  
98 Therefore, prediction should meet network control  
99 requirements about time-scale and resource utilization  
100 target. Inversely, we can evaluate traffic  
101 predictability under certain constraints, which  
102 comes from the control requirements. The result  
103 can be referred for control setup, for example, for  
104 the selection of utilization target and its related  
105 control time interval.

107 Some previous works focused on one-step traffic  
108 prediction using neural networks [13], or least  
109 mean square error (LMSE) derived SNR criterion  
110 and adaptive online traffic prediction [1]. Others  
111 includes non-stationary signal prediction investigation  
112 [8], or a general argument for the enhanced  
113 predictability with special 2nd-order traffic property  
114 like self-similarity or long-range dependence  
115 (LRD) [19,20]. Those studies, in spite of their own  
116 advantages, did not show us the efficiency of  
117 predictive traffic management, or its numerical  
118 potential under practical constraints. We expect to  
119 compensate them with this paper by answering the  
120 above questions.

121 Our method is to analyze the quantized multi-  
122 step traffic prediction uncertainty, given a complete  
123 traffic history and its stationary model as a priori  
124 knowledge. Thus, the result provides an upper  
125 bound for online prediction performance under  
126 specified error constraint or with expected  
127 prediction interval. It reveals the promising  
128 predictability of network backbone traffic (i.e. aggregated  
129 end-system traffic) or low-frequency (LF) (i.e. large  
130 time-scale) traffic variations. To answer the question  
131 of "Is the traffic predictable?" we need to take into  
132 account such factors as the net-

work control time interval, resource utilization target, traffic statistics and the measurement time-scale. In other words, how one assesses traffic predictability depends on how one wants to use the prediction results to meet the control expectation or constraint.

Next are the assumptions underlying our studies. First, we assume that all traffic traces used in this paper are stationary, their characteristics are captured by the 1st- and 2nd-order statistics, i.e. the marginal cumulative distribution function (CDF) and the power spectral density function (PSD). Furthermore, we assume that traffic can be adequately represented by a stationary model such as the auto-regressive moving average (ARMA) or Markov-modulated poisson process (MMPP).

To legitimate our analysis, we assume that the traffic modeling is reasonably accurate. It is well known that self-similarity and LRD are ubiquitous properties of network traffic, including Ethernet [21], MPEG [22] and JPEG [23] video, and WWW [24] traffic. No doubt, fractional Brownian motion (FBM) for exactly self-similar data traffic and fractional ARIMA for asymptotically self-similar video traffic are better models to capture the slowly decaying correlation function and scale-invariant burstiness. However, there are a lot of arguments about whether LRD matters in traffic management for delay-sensitive services. Being supported by [14,25–27], we argue that in a practically mission-critical control environment like ATM network, only limited traffic time-scales concern us. Therefore, ARMA and MMPP models can be used for LRD traffic since their correlation in the form of summarized exponential functions approximate the hyperbolically decaying LRD correlation.

This paper is organized as follows: Section 2 defines the constrained traffic predictability using LMSE-based optimal traffic predictor. Section 3.1 derives ARMA predictability, while Section 3.2 analyzes the effect of traffic measurement (low-pass filtering) and aggregating (multiplexing) on it. Section 3.3 examines the roles of different traffic statistics inherent in predictability. Section 3.4 gives quantitative results for ARMA-matched real traces at proper measurement time-scale and multiplexing level. Section 4 performs the analysis

with MMPP model. Section 5 is technical discussion and Section 6 concludes the paper.

## 2. Definition of traffic predictability

A network traffic is represented by a continuous-time stochastic process  $\{Y(t) = X(t) + \mu\}$ , where  $\mu$  is the mean rate, and  $\{X(t)\}$  is a purely random (regular) process with continuous integrated spectrum and zero mean. ARMA and MMPP process are all of this form. Ideally, any deterministic components can be extracted from the traffic according to the *Lebesgue decomposition theorem*, and removed from our prediction analysis.

The traffic prediction issue is illustrated in Fig. 1. It depicts the measurement-based control procedure at a finite-buffer network node, whose maximum local delay  $d_{\max}$  is typically around 30 ms. The queuing process can be characterized by the low pass filter (LPF) with cutoff frequency  $1/T_c$  [18,28], i.e. the inverse of the critical time-scale (CTS) [26]. Only the high-frequency (HF) dynamics of the input traffic are absorbed by buffering, whereas the LF part remains unchanged after buffering. Such a  $T_c$  can be used as the sampling/smoothing interval for online traffic measurement. Its engineering value ranges from  $d_{\max}$  to  $200d_{\max}$  [14]. Thus, the node can be simplified as a “bufferless” transmission system for the filtered input  $Y_L(t)$ . Its prediction-based network control, for example the dynamic bandwidth allocation or CAC, requires  $Y_L(t + \tau)$  from the measured traffic history  $\{Y_L(r) | r \in (-\infty, t]\}$ .  $\tau$  denotes the control

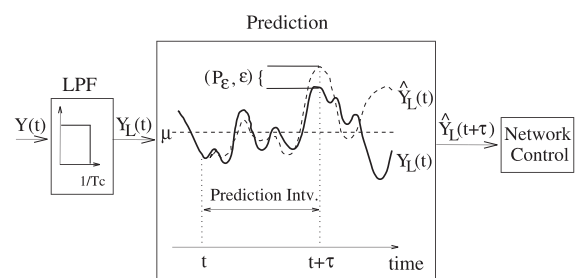


Fig. 1. Traffic prediction framework:  $Y(t)$ —arrived network traffic,  $T_c$ —filtering rate,  $Y_L(t)$ —filtered traffic rate,  $\mu$ —traffic mean rate,  $(P_e, \epsilon)$ —prediction error constraint,  $\hat{Y}_L(t + \tau)$ — $\tau$ -step predictor.

212 or prediction time interval. The result  $\hat{Y}_L(t + \tau)$ , to  
 213 be used for control purpose, is named the  $\tau$ -step  
 214 predictor. For simplicity, we neglect the subscript  
 215  $L$  in the following notations.

216 Assume the control requires that the *normalized*  
 217  $\tau$ -step prediction error ( $\overline{\text{err}}(\tau) \equiv (\hat{Y}(t + \tau) - Y(t +$   
 218  $\tau))/\hat{Y}(t + \tau)$ ) should not exceed a percentage  $\varepsilon$  (e.g.  
 219 20%) with a probability  $P_\varepsilon$  (e.g. 0.01), where  $(P_\varepsilon, \varepsilon)$   
 220 is the desired prediction confidence interval. Then  
 221 the optimal prediction performance can be char-  
 222 acterized by the maximum prediction interval  
 223 (MPI):

$$\text{MPI} \equiv \max\{\tau | P_{\overline{\text{err}}}(\tau, \varepsilon) \leq P_\varepsilon\}, \quad (1)$$

225 where  $P_{\overline{\text{err}}}(\tau, \varepsilon) = \Pr[\overline{\text{err}}(\tau) > \varepsilon]$ ;  $\overline{\text{err}}(\tau)$  is defined  
 226 from the LMSE-based optimal predictor:  $\hat{Y}(t +$   
 227  $\tau) = E[Y(t + \tau) | Y(r), -\infty < r \leq t]$ , which mini-  
 228 mizes the  $\tau$ -step variance  $\hat{\sigma}_\tau^2$  and maximizes the  
 229 signal-noise ratio  $\text{SNR}(\tau)$ , both of which will be  
 230 introduced below. Obviously a larger MPI implies  
 231 better predictability. Note that MPI includes both  
 232 the 1st- and 2nd-order statistics, while an imme-  
 233 diate judgement of good predictability upon LRD  
 234 features may only reflect the 2nd-order property.

235 If MPI accomodates enough time for measure-  
 236 ment, prediction and network control actions, and  
 237 the MPI-step prediction meets the confident re-  
 238 quirement, then the traffic of time granularity  $T_c$   
 239 would be declared predictable. In other words, the  
 240 claim is always accompanied by the measurement  
 241 time interval. An example can show us the physical  
 242 meanings of the notions: Assume the predictor is  
 243 taken as dynamically to-be-allocated bandwidth.  
 244 Then  $\overline{\text{err}}(\tau)$  denotes the bandwidth over-subscrip-  
 245 tion percentage (BOSP), while  $P_{\overline{\text{err}}}(\tau, \varepsilon)$  can be ta-  
 246 ken as the bandwidth over-subscription probability  
 247 (BOSPr).  $(P_\varepsilon, \varepsilon)$  is the required utilization target.  
 248  $\hat{Y}(t + \tau)$  is normalized by the predictor to reflect  
 249 the over-reserved portion within the allocated  
 250 bandwidth, which makes more engineering sense.  
 251 Therefore, once compared with the usually inevi-  
 252 table bandwidth re-negotiation delay, MPI tells  
 253 the feasibility to achieve the specified network ef-  
 254 ficiency. From another angle, MPI also denotes  
 255 the upper bound of the time-scale over which  
 256 bandwidth allocation can be performed accurately.

257 Equivalent to the MPI criterion, LMSE-based  
 258 SNR is another commonly used approach (see [1])

to prediction evaluation:  $\text{SNR}(\tau) = E[Y^2(t)]/\hat{\sigma}_\tau^2$ , 259  
 where  $\hat{\sigma}_\tau^2$  is the  $\tau$ -step variance of the prediction 260  
 noise  $Y(t + \tau) - \hat{Y}(t + \tau)$ , defined by  $\hat{\sigma}_\tau^2 = E[(\hat{Y}(t +$  261  
 $\tau) - Y(t + \tau))^2]$ . Later we will see the engineering 262  
 advantage of MPI over SNR. 263

### 3. Traffic predictability analysis with ARMA model 264

Gaussian processes are often used to approxi- 265  
 mate network traffic, especially backbone traffic, 266  
 where aggregation of a large number of independ- 267  
 ent sources lends credence to the model. In this 268  
 section, ARMA model is used to explore the traffic 269  
 statistical properties dominating the predictability, 270  
 and to analyze the effect of traffic smoothing and 271  
 aggregation. After that, quantitative analysis is 272  
 applied to real network traces. 273

#### 3.1. Specification of Gaussian predictability 274

First let us review the conclusions about 275  
 Gaussian prediction [11]. By *Wold's decomposition* 276  
*theorem*, any stationary regular Gaussian process 277  
 $\{Y(t) = X(t) + \mu\}$  can be uniquely represented by 278  
 an one-sided moving average of a stationary 279  
 Gaussian white noise  $\{n(t)\}$  with unit variance: 280

$$Y(t) = \int_0^{+\infty} h_u n(t - u) du + \mu, \quad (2)$$

where  $h_u$  is a real-valued function of  $u$  given a real- 282  
 valued process  $\{Y(t)\}$ . The optimal  $\tau$ -step predic- 283  
 tor of the Gaussian process  $X(t + \tau)$  is  $\hat{X}(t + \tau) =$  284  
 $E[X(t + \tau) | X(t - u), 0 \leq u < +\infty]$  in the sense of 285  
 LMSE. This predictor can be expressed as a lin- 286  
 ear form by stationary Gaussian property (*Wie-* 287  
*ner's approach*):  $\hat{X}(t + \tau) = \int_0^{+\infty} a_u X(t - u) du + b$ . 288  
 Equivalently in *Kolmogorov's approach*,  $\hat{X}(t + \tau)$  is 289  
 expressed as: 290

$$\begin{aligned} \hat{X}(t + \tau) &= \int_\tau^{+\infty} h_u n(t + \tau - u) du \\ &= \int_0^{+\infty} h_{u+\tau} n(t - u) du. \end{aligned} \quad (3)$$

A comparison between (2) and (3) tells us that the 292  
 unpredictable part in  $X(t + \tau)$  is  $\int_0^\tau h_u n(t +$  293  
 $\tau - u) du$ . So the  $\tau$ -step prediction variance  $\hat{\sigma}_\tau^2$  can 294  
 be expressed as: 295

$$\hat{\sigma}_\tau^2 = \int_0^\tau h_u^2 du = \sigma^2 - \int_\tau^{+\infty} h_u^2 du, \quad (4)$$

where  $\sigma^2$  is the variance of  $X(t)$ . Clearly,  $\hat{\sigma}_\tau^2$  is a non-decreasing function of  $\tau$ . Therefore, the further into the future one tries to predict, the more prediction error one will get. The best prediction of  $X(+\infty)$  is its mean and  $\hat{\sigma}_\infty^2 = \lim_{\tau \rightarrow +\infty} \hat{\sigma}_\tau^2 = \sigma^2$ .

Assume the rate process  $\{Y(t)\}$  is Gaussian with negligible probability for being negative. From previous definition, we can see that the  $P_{\text{err}}(\tau, \varepsilon)$  in (1) equals  $P(Z > 0)$ , the tail distribution of a Gaussian variable  $Z$  with p.d.f.  $N(-\varepsilon \cdot \mu, \sigma_{\varepsilon, \tau}^2)$ , where:

$$\sigma_{\varepsilon, \tau}^2 = \int_0^\tau h_u^2 du + \varepsilon^2 \int_\tau^{+\infty} h_u^2 du = (1 - \varepsilon^2) \hat{\sigma}_\tau^2 + \varepsilon^2 \sigma^2. \quad (5)$$

Moreover, according to (3) and (4),  $P_{\text{err}}(\tau, \varepsilon) \leq P_\varepsilon$  in (1) is equivalent to  $\sigma_{\varepsilon, \tau}^2 \leq (\varepsilon^2 \mu^2 / \phi^2(1 - P_\varepsilon))$ .  $\phi(x)$  is the inverse CDF of  $N(0, 1)$ .<sup>1</sup> Putting (5) into (1), we can get Gaussian's MPI:

$$\text{MPI} = \max \left\{ \tau \left| \frac{\hat{\sigma}_\tau^2}{\sigma^2} \leq O(P_\varepsilon, \varepsilon, C) \right. \right\}, \quad (6)$$

$$O(P_\varepsilon, \varepsilon, C) = \left[ \frac{1}{C^2 \phi^2(1 - P_\varepsilon)} - 1 \right] \frac{\varepsilon^2}{1 - \varepsilon^2}, \quad (7)$$

where  $C = \sigma/\mu$  is the variance coefficient of  $\{Y(t)\}$ . Correspondingly from the definition of  $\tau$ -step SNR, there is:

$$\text{SNR}(\tau)^{-1} = \frac{\hat{\sigma}_\tau^2}{\sigma^2} \cdot \frac{C^2}{1 + C^2}, \quad (8)$$

<sup>1</sup> Though modeling error is not our major concern in the paper, we can still roughly remove the possibly non-negligible occurrence of negative  $\hat{Y}(t + \tau)$  by adding a condition  $\hat{Y}(t + \tau) \geq 0$  to  $P_{\text{err}}(\tau, \varepsilon)$ . Then  $P_{\text{err}}(\tau, \varepsilon) \leq P_\varepsilon$  is equivalent to:

$$\frac{1}{1 - \Phi\left(\frac{-\mu}{\sqrt{1 - \hat{\sigma}_\tau^2}}\right)} \int_{-\mu/\sqrt{1 - \hat{\sigma}_\tau^2}}^{+\infty} \Phi\left(-z\varepsilon\sqrt{\frac{1}{\hat{\sigma}_\tau^2} - 1} - \frac{\varepsilon\mu}{\sqrt{\hat{\sigma}_\tau^2}}\right) \times f(z) dz \leq P_\varepsilon,$$

where  $\Phi(\cdot)$  is the CDF of  $N(0, 1)$  and  $f(z)$  is the distribution density function of  $Z \sim N(0, 1)$ .

$$\text{MPI} = \max \left\{ \tau \left| \text{SNR}(\tau)^{-1} \leq \frac{O(P_\varepsilon, \varepsilon, C) \cdot C^2}{1 + C^2} \right. \right\}. \quad (9)$$

Take a look at (6) and (7). Although the normalized prediction variance  $\hat{\sigma}_\tau^2/\sigma^2$  falls into  $[0, 1]$ , the  $\tau$ -independent  $O(P_\varepsilon, \varepsilon, C)$  can be negative when  $C > 1/(\phi^2(1 - P_\varepsilon))$  or larger than 1 upon a sufficiently large  $\varepsilon$ . In other words, MPI can be 0 upon large traffic varying amplitude ( $C$ ) or stringent BOSP ( $P_\varepsilon$ ), and be  $+\infty$  upon a large error tolerance ( $\varepsilon$ ). Obviously traffic predictability is a function of both the confidence requirement ( $P_\varepsilon, \varepsilon$ ), and the 1st- and 2nd-order statistics. It is decided by the comparison between  $P_\varepsilon$  and  $P_{\text{err}}$ , i.e. the tail distribution of  $N(-\varepsilon \cdot \mu, \sigma_{\varepsilon, \tau}^2)$ , whereas the 2nd-order traffic statistics exert influence through  $\hat{\sigma}_\tau^2$ . However,  $\lim_{\tau \rightarrow +\infty} P_{\text{err}}(\tau, \varepsilon) = \Pr[Y(t) < (1 - \varepsilon)\mu]$ . That is, the prediction effect of the infinite future is exclusively determined by the traffic tail distribution.

### 3.2. Effects of (low-pass) filtering and multiplexing on traffic predictability

In practice, traffic rate sampling (i.e. low-pass filtering) and multiplexing play critical roles in measurement-based network control or traffic engineering. Here we check their influence on traffic predictability. First, assume  $\{X(t) = Y(t) - \mu\}$  can be decomposed into  $L (> 1)$  mutually independent components:  $\{X(t)\} = \sum_{l=1}^L \{X_l(t)\}$ . Each component is still a stationary Gaussian process. A commonly used decomposition method is to filter the traffic into non-overlapping frequency regions using an ideal band-pass filter. In time domain, this corresponds to the traffic dissection at multiple time-scales. Some may argue that the decomposed processes are not regular, but they can always be transferred into regular ones by removing their deterministic components, according to *Lebesgue decomposition theorem*. The next two propositions analytically state the predictability changes after this kind of operation.

**Proposition 1.** Denote the  $\tau$ -step prediction variance of  $\{X(t)\}$  and  $\{X_l(t)\}$  as  $\hat{\sigma}_\tau^2$  and  $\hat{\sigma}_{l, \tau}^2$  respectively. Then the prediction variance of  $\{X(t)\}$  is not smaller than the sum of that of all  $\{X_l(t)\}$ :  $\hat{\sigma}_\tau^2 \geq \sum_l \hat{\sigma}_{l, \tau}^2, \forall \tau$ .

6

A. Sang, S.-q. Li / Computer Networks xxx (2002) xxx-xxx

361 **Proof.** By Wiener's approach, the optimal  $\tau$ -step  
362 predictor of  $X(t + \tau)$  is:

$$\hat{X}(t + \tau) = E[X(t + \tau)|X(t - u), 0 \leq u < +\infty]$$

$$= \int_0^{+\infty} a_u X(t - u) du + b.$$

364 To minimize the  $\tau$ -step prediction variance  $\hat{\sigma}_\tau^2$   
365 as required by the LMSE criterion, the optimal pa-  
366 rameters  $a_u (\forall u)$  and  $b$  satisfy the well-known  
367 Wiener-Hopf equations:  $\forall v \in [0, +\infty)$ ,

$$\int_0^{+\infty} C_X(t - u, t - v) a_u du = C_X(t + \tau, t - v),$$

$$b = E[X(t + \tau)] - \int_0^{+\infty} a_u E[X(t - u)] du = 0,$$

369 where  $C_X(\cdot, \cdot)$  is the auto-correlation function of  
370  $\{X(t)\}$ . Due to the optimal  $a_u$  and  $b$  and the fact  
371 that  $E[(X(t + \tau) - \hat{X}(t + \tau))\hat{X}(t + \tau)] = 0$ , the  
372 minimized  $\hat{\sigma}_\tau^2$  is:

$$\hat{\sigma}_\tau^2 = \sigma^2 - \int_{u=0}^{+\infty} \int_{v=0}^{+\infty} C_X$$

$$\times (t - v, t - u) a_u a_v dv du. \quad (10)$$

374 In fact this equation also holds for every  $\{X_l(t)\}$   
375 with corresponding  $\hat{\sigma}_{l,\tau}^2$ ,  $\sigma_l^2$ ,  $C_{X_l}(\cdot, \cdot)$  and  $(a_{l,u}, b_l)$ .<sup>2</sup>  
376 Because of the independent decomposition, it fol-  
377 lows:

$$\sigma^2 = \sum_{l=1}^L \sigma_l^2 \quad \text{and} \quad C_X(\cdot, \cdot) = \sum_{l=1}^L C_{X_l}(\cdot, \cdot).$$

379 Therefore,

$$\hat{\sigma}_\tau^2 = \sum_{l=1}^L \left( \sigma_l^2 - \int_{u=0}^{+\infty} \int_{v=0}^{+\infty} C_{X_l}(t - v, t - u) a_{u,l} a_{v,l} dv du \right)$$

$$\geq \sum_{l=1}^L \left( \sigma_l^2 - \int_{u=0}^{+\infty} \int_{v=0}^{+\infty} C_{X_l}(t - v, t - u) a_{u,l} a_{v,l} dv du \right)$$

$$= \sum_{l=1}^L \hat{\sigma}_{l,\tau}^2,$$

381 because it is  $(a_{u,l}, a_{v,l})$ , instead of  $(a_u, a_v)$ , uniquely  
382 minimizes  $\hat{\sigma}_{l,\tau}^2$ . If the decomposition is i.i.d., then  
383 we can show that  $\forall \tau$ ,  $\hat{\sigma}_\tau^2 = \sum_{l=1}^L \hat{\sigma}_{l,\tau}^2$ .  $\square$

<sup>2</sup> Please note that the  $C_X(\cdot, \cdot)$  and  $C_{X_l}(\cdot, \cdot)$  here are independent of  $t$  for their stationarity, whereas  $(a_u, b)$  and  $(a_{l,u}, b_l)$  are functions of  $\tau$ .

**Proposition 2.** Denote the MPI of  $\{Y(t) = X(t) + \mu\}$  and  $\{Y_l(t) = X_l(t) + \mu\}$  as  $\tau^*$  and  $\tau_l^*$  respectively, within the same prediction confidence interval  $(P_\varepsilon, \varepsilon)$ . Then the MPI of  $\{Y(t)\}$  is not larger than the minimum one among MPIs of all  $\{Y_l(t)\}$ :  $\tau^* \leq \min_l \tau_l^*$ .

**Proof.** Assume  $\tau^* > \tau_l^*$ . For the optimal prediction of a Gaussian process from a complete history,  $\hat{\sigma}_\tau^2$  is a non-decreasing function of  $\tau$ . With the conclusion of Proposition 1, we can get:  $\hat{\sigma}_{\tau^*}^2 \geq \hat{\sigma}_{\tau_l^*}^2 \geq \hat{\sigma}_{l,\tau_l^*}^2$ . However, by (6) and (7),  $\hat{\sigma}_{\tau^*}^2 \geq \hat{\sigma}_{l,\tau_l^*}^2$  implies  $\sigma^2 \leq \sigma_l^2$ , which is surely impossible.  $\square$

Proposition 1 tells us that the prediction of a purely random (Gaussian) process is not better than that of any of its independently-decomposed components. Proposition 2 suggests that the (ideal) low-pass filtering, which keeps traffic mean rate intact, improves the predictability. Intuitively, a LPF slows down traffic changes by removing small time-scale variations (HF randomness) from the traffic, thus brings a more predictable traffic behavior. The more randomness one filters out, the better result one can get. In an extreme case, if only the DC term  $\mu$  were left after filtering, it would have an unlimited predictability.

Next we will check the effect of traffic statistical multiplexing on its predictability. Assume  $\{Y(t)\}$  is the superposition of  $M$  i.i.d. Gaussian processes  $\{Y_m(t) = X(t) + \mu\}$  ( $m = 1, 2, \dots, M$ ). After the aggregation, the  $O(P_\varepsilon, \varepsilon, C)$  in Eq. (7) increases because  $C^2$  is scaled up with  $M$ . However,  $\hat{\sigma}_\tau^2/\sigma^2$  remains unchanged because  $\hat{\sigma}_\tau^2$  and  $\sigma^2$  increase with the same scale by (4). Therefore, it can be seen clearly from (6) that traffic multiplexing increases MPI, and thus improves predictability. This fact reveals that generally a better prediction can be expected for aggregated traffic sources, compared to that for each individual one. In addition, a high-level multiplexing (i.e. a big  $M$ ) can make the  $O(P_\varepsilon, \varepsilon, C)$  larger than one by scaling down  $C$ . If so, the aggregated source would have an unlimited predictability in the sense that the prediction of its any future would never violate the  $(P_\varepsilon, \varepsilon)$  requirement.

Although not proved, we believe that the above conclusions also hold for a self-similar traffic. The

430 traffic, if investigated at limited but meaningful  
431 time-scales, may be predicted more easily than at  
432 all time-scales simultaneously. On the other hand,  
433 multiplexing reduces the traffic fluctuation ampli-  
434 tude around its mean rate, i.e. even if the 2nd-order  
435 order burstiness (denoted by a *Hurst parameter*  
436 larger than 0.5) remains similar. Later the con-  
437 clusions will be verified by quantitative analysis of  
438 real traffic traces.

### 439 3.3. Roles of traffic properties in traffic predictabil- 440 ity

441 What traffic properties characterize the inherent  
442 traffic predictability? By [16,17], traffic statistics of  
443 orders higher than two has little effect on queuing  
444 performance. Therefore, we will use the Gaussian  
445 traffic process of a bell-shaped power spectrum for  
446 analysis in that it provides a decomposable sta-  
447 tistical structure.

448 With this help, we first show that the half-power  
449 PSD bandwidth plays a more fundamental role in  
450 determining traffic predictability than other 2nd-  
451 order statistics, such as the central frequency of  
452 PSD bells. In other words, the PSD spectrum  
453 dispersion has more side effect on predictability  
454 than the PSD frequency location. In time domain,  
455 it is identical to the number of traffic correlation  
456 time-scales verse specific time-scale sizes. The more  
457 time-scales a traffic process is correlated at, the  
458 harder it can be predicted. This holds no matter  
459 whether the time-scales are all big or all small.  
460 Induced from this point, the correlation time-scale  
461 abundance across a wide range, as a property of  
462 most network traffics, has a negative effect on  
463 predictability.

464 Furthermore, we find that a narrow-banded  
465 traffic is relatively easier to predict, and wide-ban-  
466 ded PSD components contribute more to the total  
467 prediction error. Thus, LRD traffic, corresponding  
468 to the one of narrow-banded PSD that follows the  
469 power law when approximating zero frequency,  
470 tends to be easier to predict than short-range de-  
471 pendence (SRD) traffic. The SRD component of a  
472 traffic is the main hurdle to its good predictability.

473 Finally, we show that among the 1st-order  
474 traffic statistics, the CDF tail behavior accounts  
475 the most for traffic predictability, while the vari-

476 ance coefficient reflects predictability in a  
477 straightforward way. The analysis follows.

478 Assume the power spectrum and auto-correla-  
479 tion function of  $\{Y(t)\}$  are respectively [16]:  
480

$$P(\omega) = 2\pi\mu^2\delta(\omega) + \sum_{l=1}^{N-1} \frac{\psi_l(-2\lambda_l)}{\lambda_l^2 + \omega^2},$$

$$R(t) = \mu^2 + \sum_{l=1}^{N-2} \psi_l e^{\lambda_l |t|},$$

481 where  $N$  is the eigenvalue number;  $\mu^2$  is the DC-  
482 term of a zero eigenvalue;  $\psi_l$  is the corresponding  
483 power vector of eigenvalue  $\lambda_l$ . Each pair of  $(\psi_l, \lambda_l)$   
484 forms a bell-shaped component in PSD. Each bell  
485 has a half-power PSD bandwidth  $BW_l = -2\text{Re}(\lambda_l)$   
486 and central frequency  $\omega_l = \text{Im}(\lambda_l)$ . From the *ca-*  
487 *nonical factorization* of PSD, we can get the  
488 unique transfer function of the ARMA process as  
489  $H(s) = \int_0^{+\infty} h_u e^{-su} du$ , which is equivalent to  
490  $X(t) = \int_0^{+\infty} h_u n(t-u) du$ . Then  $\hat{\sigma}_\tau^2$  can be derived  
491 from (4).  
492

493 For simplicity, let us consider the prediction of  
494 an ARMA(2,1) process with the assumption of  
495  $\lambda_1 = \lambda_2^* \equiv \lambda e^{j\omega}$  and  $\psi_1 = \psi_2^* \equiv \psi e^{j\beta}$ . After a com-  
496 plex PSD factorization, we get:

$$\frac{\hat{\sigma}_\tau^2}{\sigma^2} = 1 - e^{-BW\tau} + e^{-BW\tau} \times \left[ 1 + \sin(2\omega\tau) \tan \beta - \cos(2\omega\tau) - \frac{1 - \cos(2\omega\tau)}{\cos \beta \left( \cos \beta + \sqrt{\left(\frac{BW}{2\lambda}\right)^2 - \sin^2 \beta} \right)} \right], \quad (11)$$

497 where  $\sigma^2 = 2\psi \cos \beta$  is the variance of the process.  
498 A numerical study tells us that the PSD bell  
499 bandwidth (BW), central frequency ( $\omega$ ) and phase  
500 ( $\beta$ ) have similar roles in predictability as in auto-  
501 correlation function  $R(\tau) = 2\psi e^{-(BW/2)|\tau|} \cos(\omega|\tau| + \beta)$ . To some extent,  $R(\tau)$  characterizes traffic pre-  
502 dictability if the 1st-order statistics are fixed.  
503

504 Using the ARMA(2,1) as an example, Figs. 2  
505 and 3 illustrate the roles of BW,  $\omega$  and  $C$  in its  
506 predictability with  $\beta = 0$  for simplicity. It is obvi-  
507

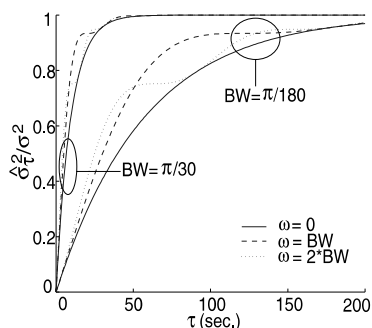


Fig. 2. Normalized prediction variance as a function of  $\tau$ .

ous that  $\hat{\sigma}_\tau^2/\sigma^2$  increases with  $\tau$ , reflecting more prediction uncertainty over larger prediction interval. BW denotes the exponentially decaying rate of traffic predictability, and  $\omega$  represents its oscillation frequency. In frequency domain, it is the PSD bandwidth, not the central frequency, that dominates traffic predictability. In another viewpoint, a wide PSD bandwidth implies large spectrum dispersion, thus abundant traffic randomness, and consequently poor traffic predictability. In extreme cases, a white noise which has an infinite BW and zero MPI, or a sinusoidal process which has a zero BW and an infinite MPI, makes the argument intuitive. In addition, as illustrated by Fig. 3(b), a small  $C$ , coming from a big mean (1st-order) or a small variance (2nd-order), reflects a smooth traffic, and therefore better predictability. In the figure, 0.086 is the lower bound of  $C$  to ensure  $O(P_\varepsilon, \varepsilon, C)$  less than one.

Take aggregated voice sources for example. Each voice source can be characterized by an on-off model whose average talkspurt and silence

period are 0.4 and 0.6 s respectively [4]. The input rate during talkspurt period is 32 Kbps (i.e. 75.5 cells/s). A T1 link with a 300-cell buffer can support 98 voice channels with average cell loss rate less than  $10^{-5}$ . It is calculated by solving the finite quasi-birth-death (QBD) distribution for the T1 queuing system using the Folding algorithm [15]. The superposition of  $M$  i.i.d. voice sources (an MMPP process) has a single-bell PSD of  $(BW, \omega) = (2(1/0.4 + 1/0.6), 0)$  and  $C = \sqrt{0.6/0.4M}$ . Detailed derivations can be referred to [16]. In addition, the aggregate source can be approximated by a first order ARMA process, especially when  $M$  is big (98, say). From canonical factorization and (6), we get:

$$\frac{\hat{\sigma}_\tau^2}{\sigma^2} = 1 - e^{-BW\tau}, \quad \text{MPI} = \frac{1}{(-BW)} \ln[1 - O(P_\varepsilon, \varepsilon, C)].$$

The MPI is depicted in Fig. 4(a), where the dotted lines denote the upper limits of  $M$  to make  $O(P_\varepsilon, \varepsilon, C)$  equal to one, and MPI infinity. For example, when  $(P_\varepsilon, \varepsilon)$  is (0.01, 20%),  $\text{MPI} = [29, 156, 770 \text{ ms}]$  for  $M = [50, 150, 203]$ . However, MPI is infinity as  $M \geq 204$ . Furthermore, if  $(P_\varepsilon, \varepsilon)$  is relaxed from (0.01, 20%) to (0.1, 20%), we get  $\text{MPI} = [76, 599 \text{ ms}]$  for  $M = [30, 61]$ , and MPI is infinity for  $M \geq 62$ . The intuition behind this is: for a high degree of traffic aggregation, or a loose error constraint, the prediction scheme reduces to the estimation of the deterministic mean rate, which results in an infinite MPI. The two points (“o” and “x”) in the figure shows that for the T1 system, prediction interval of the aggregated voice channels can not be larger than 269 or 74 ms with the confidence interval of (0.1, 15%) or (0.01, 20%)

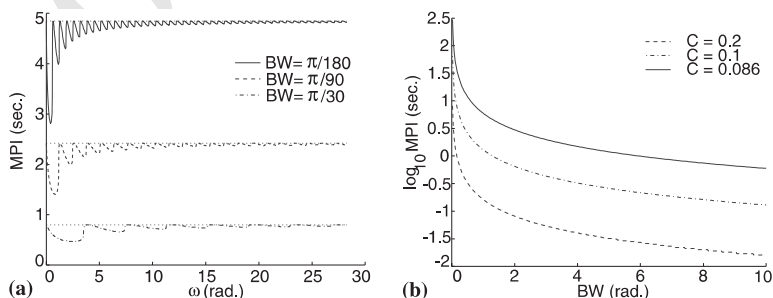


Fig. 3. Effect of PSD factors and  $C$  on MPI at  $(P_\varepsilon, \varepsilon) = (0.01, 20\%)$ : (a)  $C = 0.25$ , (b)  $\omega = 0$ .



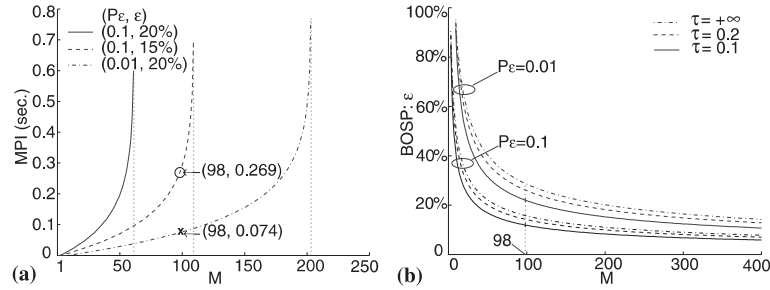


Fig. 4. ARMA prediction of  $M$  i.i.d. multiplexed Voice channels: (a) predictability, (b)  $\epsilon$ :  $\Pr\{\overline{\text{err}}(\tau) > \epsilon\} = P_\epsilon$ .

563 respectively. It means that we can not confidently  
 564 predict the rate of next talkspurt, not even for the  
 565 aggregate source! We can, however, confidently  
 566 predict the infinite future if  $(P_\epsilon, \epsilon)$  is relaxed to (0.1,  
 567 20%)! On the other hand, if 1 s's future is to be  
 568 predicted, only the right regions to the  $M$  limits  
 569 (see Fig. 4(a)) are "predictable" for corresponding  
 570 confidence requirements. Nevertheless, the results  
 571 here are for unfiltered voice traffic.

572 Fig. 4(b) shows the  $(1 - P_\epsilon)$ -percentile limit of  
 573 prediction error, i.e. the upper bound of the  
 574 bandwidth resource set aside (as BOSP) to absorb  
 575 the error: With probability  $P_\epsilon$ ,  $\overline{\text{err}}(\tau)$  may exceed  
 576 its limit  $\epsilon$ . Equivalently, with probability  $1 - P_\epsilon$ ,  $\epsilon$   
 577 upper bounds the reserved bandwidth resource  
 578 (BOSP). In other words, prediction-based network  
 579 control can expect a higher bandwidth utilization  
 580  $(1 - \text{BOSP})$  with increasing aggregation level ( $M$ ).

### 581 3.4. Predictability studies for real traffic traces

582 In this section, we analyze the predictability of  
 583 some real network traces sampled and aggregated  
 584 at different scales. A sliding window of size  $T_c$  is  
 585 used as the LPF for traffic sampling, where  $T_c$   
 586 takes empirical engineering values. Prony method  
 587 [10], which works well with the absence of noise, is  
 588 used to estimate and identify an ARMA process  
 589 for the sampled traffic traces. Consequently,  $\hat{\sigma}_\tau^2$   
 590 and MPI can be obtained from (4) and (7) re-  
 591 spectively. The 99-percentile traffic predictability,  
 592 i.e. with  $P_\epsilon$  fixed as 0.01, is presented. The nu-  
 593 merical results verify previous analysis, and show  
 594 upper bounds for the optimal performance of  
 595 online prediction.

The traces used here are Internet [5], Ethernet 596  
 [2], MPEG-1 [12] and JPEG [6], with very different 597  
 characteristics by reference. The Internet is the 598  
 Fixwest trace of a length 1084 s and a mean rate 599  
 26.32 Mbps. The Ethernet is the LAN traffic (BC- 600  
 pAug89) of 3142.83 s and 1.105 Mbps respectively. 601  
 The MPEG-1 is a Starwar video trace of 3600 s 602  
 and 0.334 Mbps. The JPEG is a segment (the slice 603  
 10–19) of Starwar video trace of 1187 s and 5.272 604  
 Mbps. The variance coefficient is shown in (a)'s of 605  
 Figs. 5–8 respectively. To get a good match (of the 606  
 LF PSD especially), the ARMA model's order is 607  
 selected carefully. For instance, the Internet trace 608  
 is well matched by ARMA(23,22), ARMA(15,14) 609  
 and ARMA(3,2) when  $T_c = 1, 4$  and 10 s respec- 610  
 tively. The higher order reflects more exponential 611  
 components needed to capture the more traffic 612  
 correlation time scales because of the finer sam- 613  
 pling granularity. 614

615 From the (a)'s of Figs. 5–8, we can see clearly 616  
 that larger traffic (measurement) time-scale derives 617  
 better predictability. In addition,  $\hat{\sigma}_\tau^2/\sigma^2$  monoton- 618  
 ically increases with  $\tau$ , reflecting the deteriorating 619  
 prediction precision with expanding prediction 620  
 interval. The MPI of single trace is shown in Table 621  
 1, where 0.01 represents the numerical precision, 622  
 and 0 occurs when  $O(P_\epsilon, \epsilon, C)$  in (6) is negative. By 623  
 the numbers, the predictability of end-system 624  
 traffics, such as the Ethernet, JPEG and MPEG-1, 625  
 is not encouraging in that their MPIs are even less 626  
 than the sampling interval! In other words, we 627  
 cannot even confidently predict the next step of the 628  
 sampled traces, even all of them have a self-similar 629  
 structure. Although contrary to our expectation, 630  
 we believe it is a natural result from the prediction

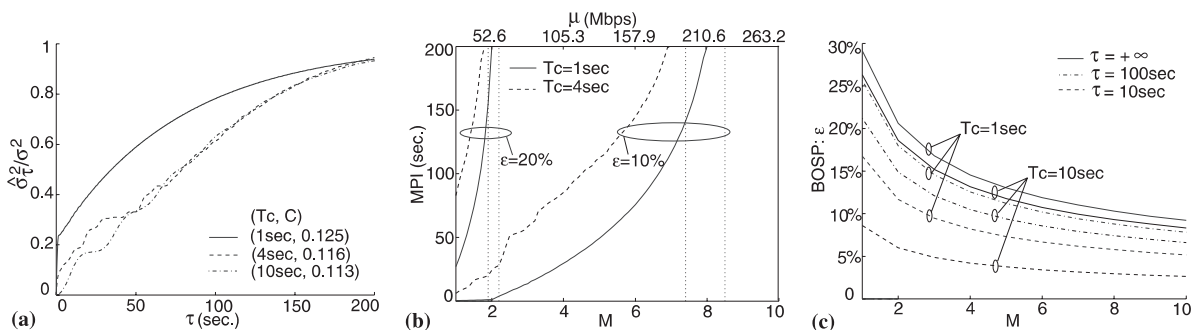


Fig. 5. ARMA-matched Internet trace: (a) normalized prediction variance, (b) MPI, (c)  $\epsilon: \Pr[\overline{\text{err}}(\tau) > \epsilon] = P_\epsilon$ .

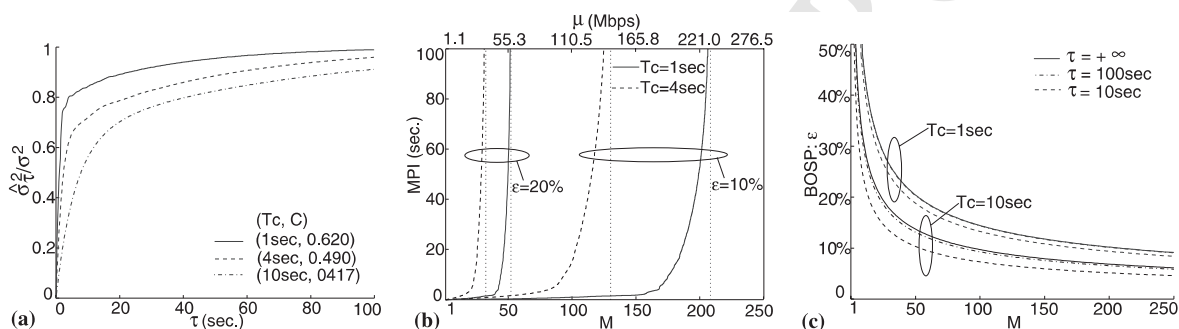


Fig. 6. ARMA-matched Ethernet trace: (a) normalized prediction variance, (b) MPI, (c)  $\epsilon: \Pr[\overline{\text{err}}(\tau) > \epsilon] = P_\epsilon$ .

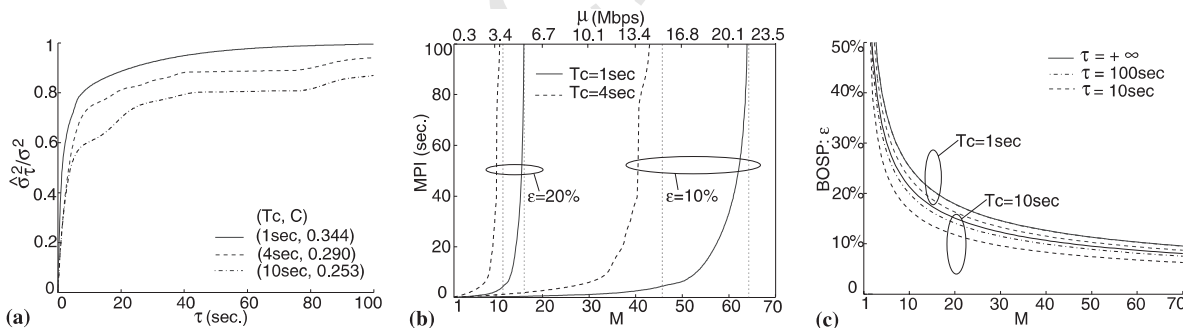


Fig. 7. ARMA-matched MPEG-1 trace: (a) normalized prediction variance, (b) MPI, (c)  $\epsilon: \Pr[\overline{\text{err}}(\tau) > \epsilon] = P_\epsilon$ .

631 definition as a function of  $C$ , the 2nd-order correlation statistics, and the tight confidence interval  
 632 with practical engineering and control meanings.  
 633 For Ethernet, its CSMA/CD mechanism and the unpredictable source interaction may explain this.  
 634 For JPEG and MPEG-1 video, the bursty scene changes and the non-stationary pseudo-periodic  
 635 (MPEG I-B-P) frame size variations account for  
 636  
 637  
 638

the poor online predictability. Comparatively,  
 639 JPEG exhibits better predictability than MPEG-1  
 640 and Ethernet, as implicitly indicated by its smaller  
 641  $C$  and thus a smoother behavior.  
 642

In contrast, Internet prediction has much better  
 643 results for the multiplexing gain, therefore implies  
 644 more potential usage in reality. As further proved  
 645 by the (b)'s of Figs. 5–8, traffic aggregation im-  
 646

639  
 640  
 641  
 642  
 643  
 644  
 645  
 646

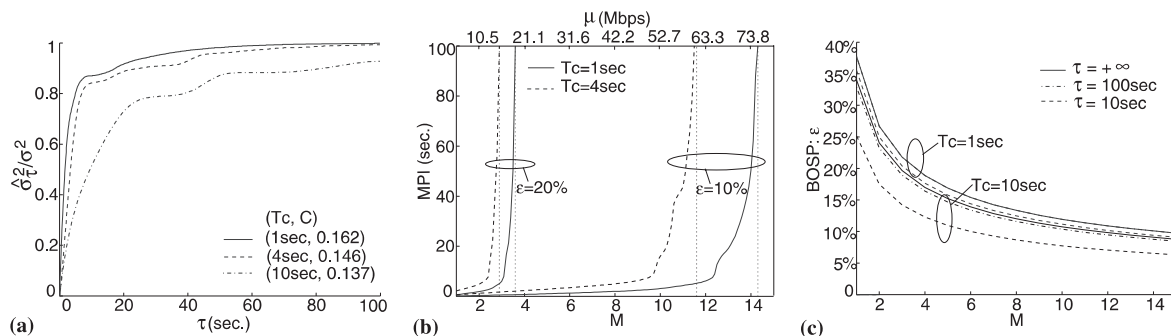


Fig. 8. ARMA-matched JPEG trace: (a) normalized prediction variance, (b) MPI, (c)  $\epsilon: \Pr[\overline{\text{err}}(\tau) > \epsilon] = P_\epsilon$ .

Table 1  
ARMA-based MPI (s) for single trace,  $P_\epsilon = 0.01$

$\epsilon$	$T_c$ (s)	MPEG-1	JPEG	Ethernet	Internet
10%	1	0.01	0.12	0	0.41
	4	0.05	0.57	0	6.09
	10	0.08	0.88	0.01	12.79
20%	1	0.04	0.67	0	27.08
	4	0.21	2.09	0	83.03
	10	0.35	5.54	0.05	89.68

647 proves traffic predictability, where MPI are ob-  
648 tained for  $M$  i.i.d. multiplexed sources while pre-  
649 diction error is limited by  $(P_\epsilon, \epsilon)$ . For each specified  
650  $T_c$  and  $\epsilon$ , the dotted line denotes the limit of  $M$  to  
651 reach an infinite MPI.

652 Usually we are more interested in the predict-  
653 able time-scale of aggregated traces in real scen-  
654 arios, where link speed allows reasonable level of  
655 traffic multiplexing. Table 2 presents this with the  
656 MPI of i.i.d. multiplexed traces at OC-1 and OC-3  
657 link level. It is observed that at reasonable aggrega-  
658 tion level, pure MPEG-1 or JPEG also demon-

Table 2  
ARMA-based MPI (s) for i.i.d. multiplexed traces,  $(P_\epsilon, \epsilon) = (0.01, 10\%)$

Load level	$T_c$ (s)	MPEG-1	JPEG	Ethernet	Internet
Mean at	1	$+\infty$	3.08	0.59	1.22
	4	$+\infty$	16.04	1.37	24.18
	10	$+\infty$	$+\infty$	7.60	39.96
OC-1	1	$+\infty$	$+\infty$	1.61	75.94
	4	$+\infty$	$+\infty$	$+\infty$	144.89
	10	$+\infty$	$+\infty$	$+\infty$	160.83

659 strates good predictability. The Internet and  
660 Ethernet has poorer predictability simply because  
661 of the less multiplexing gain for smaller source  
662 numbers. Generally speaking, much better pre-  
663 dictability can be expected for network backbone  
664 traffic that bears heavily multiplexed end-system  
665 sources, in contrast to a single end-system traffic  
666 source. Still, the sampling interval plays a crucial  
667 role in the assessment.

668 The (c)'s of Figs. 5–8, depict the upper bound ( $\epsilon$ )  
669 of the prediction error ( $\overline{\text{err}}(\tau)$ ) as before. They  
670 demonstrate the tradeoff between small BOSP (i.e.  
671 small bandwidth loss) and large control interval.  
672 In Fig. 5(c) for example, assume  $\epsilon = 30\%$  is an  
673 affordable utilization loss, the prediction-based  
674 Internet traffic engineering would be feasible for  
675 the remotest future. Usually, per-flow traffic pre-  
676 diction is too costly to benefit control purposes.  
677 Therefore, it has more limited usage than aggrega-  
678 ted traffic prediction. Yet, a carefully selected  $T_c$   
679 may help both cases.

680 To get more insights to our predictability crite-  
681 rion MPI, we calculate the BOSP and the inverse  
682 SNR for 1-step traffic prediction in Table 3. As we  
683 discussed before, MPI and SNR are two equivalent  
684 criteria in the sense of LMSE. The table shows the  
685 lower bounds of online prediction noise from two  
686 different angles. Network controller may select ei-  
687 ther one for evaluation. However, we can see  
688 clearly from the table that the small  $\text{SNR}^{-1}$  actu-  
689 ally gives an over-optimistic, if not misleading,  
690 impression about online traffic predictability. The  
691 next example shows how the BOSP and  $\text{SNR}^{-1}$   
692 form the bounds of the optimal online prediction

Table 3  
ARMA-based 1-step ( $\tau = T_c$ ) prediction error for single trace

Error measure	$T_c$ (s)	MPEG-1	JPEG	Ethernet	Internet
BOSP	1	65.1%	23.1%	376.8%	15.5%
	4	55.9%	26.6%	128.2%	9.4%
	10	49.3%	23.5%	95.1%	8.6%
SNR <sup>-1</sup>	1	0.043	0.009	0.156	0.004
	4	0.042	0.012	0.115	0.002
	10	0.036	0.010	0.083	0.001

693 performance: In paper [1], the adaptive LMSE  
694 approach is used to predict the 1-step GOP rate of  
695 the Starwar MPEG video in real time. The value of  
696 SNR<sup>-1</sup> was computed as 0.068 in that paper. It is  
697 larger than the lower bound (0.043) given in our  
698 table, where ARMA prediction is armed with a  
699 complete traffic history and stationarity assumption  
700 as well. On the other hand, if  $\varepsilon = 10\%$  and set  
701 0.068 as the maximum SNR<sup>-1</sup>, MPI would be 2.95  
702 s by (6) and (8). This value is surely an upper bound  
703 of the one-step ( $\tau = 1$  s) prediction interval in [1].

#### 704 4. Traffic predictability analysis with MMPP model

705 Up to now, we have examined traffic predict-  
706 ability using ARMA model. Will the conclusions  
707 be consistent if the MMPP is used instead? By our  
708 previous research [17], circulant Markov-modu-  
709 lated poisson process (CMPP) being a special  
710 MMPP can be used to match real traces. It cap-  
711 tures not only the 2nd-order statistics, just as  
712 ARMA does, but also the 1st-order statistics even  
713 of a non-Gaussian distribution. This model per-  
714 forms well in queuing analysis by our previous  
715 research [17].

##### 716 4.1. Specification of CMPP predictability

717 First take a look at the CMPP properties [17].  
718 CMPP process  $\{Y(t)\}$  has a rate vector  
719  $\vec{r} = [r_1, \dots, r_i, \dots, r_N]$  and a  $N$ -state circulant  
720 transition matrix  $Q$ . The steady-state probability  
721 of this process is  $1/N$  for all states. In addition,  
722 there is the decomposition of  $Q = \mathbf{F}\mathbf{A}\mathbf{F}^*$ , where  $\mathbf{F}$  is  
723 a Fourier matrix with the  $(i, j)$ th element as

$W^{ij} = \frac{1}{\sqrt{N}} e^{(-2\pi(i-1)(j-1)/N)\sqrt{-1}}$ ,  $\mathbf{F}^*$  is the conjugate  
transpose of  $\mathbf{F}$ , and  $\mathbf{A} = \text{diag}[\lambda_1, \dots, \lambda_i, \dots, \lambda_N]$ .  
All eigenvalues in  $\mathbf{A}$  have a negative real part ex-  
cept  $\lambda_1 = 0$ . Assume  $Y(t) = r_i$ , then the probability  
for  $Y(t + \tau) = r_j$  should be  $[e^{Q\tau}]_{ij}$ , i.e. the  $(i, j)$ th  
element of the transition probability matrix  $[e^{Q\tau}]$ .

By Markov property, the optimal predictor for  
 $Y(t + \tau)$  is:

$$\begin{aligned} \hat{Y}_i(t + \tau) &\equiv E[Y(t + \tau)|Y(t) = r_i] \\ &= \sum_{k=1}^N r_k [e^{Q\tau}]_{ik} \\ &= \frac{1}{N} \sum_{k=1}^N r_k \sum_{l=1}^N e^{\lambda_l \tau} W^{l(i-k)}. \end{aligned} \quad (12)$$

Therefore a conditional BOSPr, the prediction  
error probability subject to the initial state of  
 $Y(t) = r_i$ , can be written as:

$$P_{\text{err}_i}(\tau, \varepsilon) = \Pr[\overline{\text{err}}_i(\tau) > \varepsilon | Y(t) = r_i] = \sum_{\{j\}_i^*} [e^{Q\tau}]_{ij},$$

where  $\{j\}_i^* = \{j | r_j < (1 - \varepsilon)\hat{Y}_i(t + \tau)\}$ , and  
 $\overline{\text{err}}_i(\tau) = (\hat{Y}_i(t + \tau) - Y(t + \tau))/\hat{Y}_i(t + \tau)$ . By (1),  
the  $(1 - P_e)$ -percentile CMPP predictability is:

$$\begin{aligned} \text{MPI} &= \max\{\tau | P_{\text{err}}(\tau, \varepsilon) < P_e\}, \quad \text{where } P_{\text{err}}(\tau, \varepsilon) \\ &= \frac{1}{N} \sum_{i=1}^N P_{\text{err}_i}(\tau, \varepsilon) = \frac{1}{N} \sum_{i=1}^N \sum_{\{j\}_i^*} [e^{Q\tau}]_{ij}. \end{aligned} \quad (13)$$

$P_{\text{err}}(\tau, \varepsilon)$  is the steady-state BOSPr for predict-  
ing  $Y(t + \tau)$  from  $Y(t)$ . By (12), there is  
 $\forall i, \lim_{\tau \rightarrow +\infty} \hat{Y}_i(t + \tau) = \mu$ . Furthermore,  $\lim_{\tau \rightarrow +\infty} \times$   
 $P_{\text{err}}(\tau, \varepsilon) = \lim_{\tau \rightarrow +\infty} P_{\text{err}_i}(\tau, \varepsilon) = \Pr[Y(t) < (1 - \varepsilon)\mu]$ .  
Therefore, prediction performance of the infinite  
future again depends only on the 1st-order statis-  
tics of the traffic.

When  $M$  MMPP sources  $(Q_m, \vec{r}_m)$  ( $m = 1, 2, \dots,$   
 $M$ ) are multiplexed together, the aggregate source  
is also an MMPP with  $(Q, \vec{r})$  given by:

$$Q = Q_1 \oplus Q_2 \oplus \dots \oplus Q_M, \quad \vec{r} = \vec{r}_1 \oplus \vec{r}_2 \oplus \dots \oplus \vec{r}_M,$$

where  $\oplus$  is the Kronecker sum operator. However,  
the state number of the aggregate source may ex-  
plode into the product of the state numbers of all  
the  $M$  sources. To avoid this, the CDF of the ag-  
gregate source is first obtained from the convolu-  
tion of the CDFs of all the  $M$  sources, then it is

758 quantified with a reasonable state number  $N$ , at  
 759 the cost of a granularity loss with the resulted rate  
 760 vector. The CMPP modeling procedure can be  
 761 done by the SMAQ tool [17].

#### 762 4.2. Predictability studies for real traffic traces

763 This section examines traffic predictability for  
 764 CMPP-matched real traces. Using the Internet  
 765 traffic as an example, Fig. 9 shows that CMPP and  
 766 ARMA can capture the PSD of real traces equally  
 767 well (where the solid line merges with the dashed  
 768 line), but CMPP has a better match of the CDF  
 769 than ARMA (where the dashed line merges with the  
 770 dotted line). In Fig. 10(a), the steady-state  
 771 BOSPr increases with  $\tau$ , reminding us of the  
 772 tradeoff between a large  $\tau$  and a small prediction  
 773 error. Fig. 10(b) again confirms the beneficial effect  
 774 of low-pass filtering and multiplexing on traffic  
 775 predictability as before.

776 There are obvious numerical differences between  
 777 the prediction of CMPP (Tables 4 and 5) and

778 ARMA (Tables 1 and 2). It comes from the  
 779 modeling change, especially the different matching  
 780 effect of the traffic tail distribution. In spite of that,  
 781 the MPI values from both models are approxi-  
 782 mately at the same scale to upper bound the fea-  
 783 sible prediction intervals. By Tables 4 and 5,  
 784 CMPP analysis shows the same picture about the  
 785 predictability of single end-system traffic verses  
 786 Internet backbone traffic or aggregate end-system  
 787 sources. Again, the sampling interval greatly af-  
 788 fects the assessment.

#### 789 5. Discussion

790 Previously we used (BOSPr, BOSP) to measure  
 791 the prediction cost in terms of the over-subscribed  
 792 bandwidth resource. Actually there is a symmetric  
 793 possibility for bandwidth under-subscription to  
 794 occur. Take a further look at the predictability  
 795 definition in Section 3.1. The predictor  $\hat{Y}(t + \tau)$   
 796 there has the same mean value as  $Y(t + \tau)$ , but a

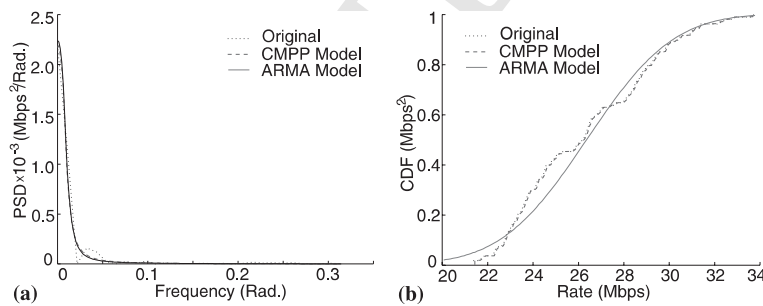


Fig. 9. The matching effect of the Internet trace,  $T_c = 10$  s: (a) PSD matching (b) CDF matching.

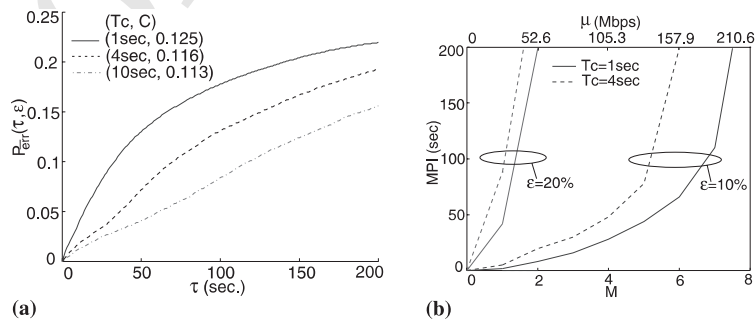


Fig. 10. CMPP-matched Internet trace: (a) steady-state BOSPr,  $\epsilon = 10\%$  (b) MPI with  $P_\epsilon = 0.01$ .

Table 4  
CMPP-based MPI (s) for single trace,  $P_e = 0.01$

$\varepsilon$	$T_c$ (s)	MPEG-1	JPEG	Ethernet	Internet
10%	1	0.07	0.09	0.02	1.8
	4	0.13	0.26	0.02	5.2
	10	0.14	1.04	0.03	8.4
20%	1	0.08	0.28	0.03	41.7
	4	0.26	2.40	0.05	88.2
	10	0.43	8.30	0.19	$+\infty$

Table 5  
CMPP-based MPI (s) for i.i.d. multiplexed traces,  $(P_e, \varepsilon) = (0.01, 10\%)$

Load level	$T_c$ (s)	MPEG-1	JPEG	Ethernet	Internet
Mean at	1	$+\infty$	2.8	0.24	8.3
OC-1	4	$+\infty$	49.8	1.20	19.7
	10	$+\infty$	$+\infty$	15.06	21.3
Mean at	1	$+\infty$	$+\infty$	6.78	65.9
OC-3	4	$+\infty$	$+\infty$	$+\infty$	$+\infty$
	10	$+\infty$	$+\infty$	$+\infty$	$+\infty$

797 smaller variance. It means that the predictor process is smoother compared to the predicted process, which explains why the predicted rate “peak” tends to be lower than the actual value, but the predicted rate “valley” tends to be higher. This phenomenon is often seen in applications of ARMA prediction. It may upset the network controller who is seeking for an accurate peak rate prediction. For instance, in measurement-based CAC (MCAC), the peak traffic rate in the next control time interval, which is upper bounded by  $\tau$ , is usually estimated from an observed history with limited length  $T_m$ . The result is taken as the future traffic load for CAC purposes. Previous research mainly focused on  $T_m$ , as did by [7]. Ref. [9] estimates traffic load for the next control interval  $T$  based on the peak rate in the past interval, but  $T$  is only empirically fixed. As an improvement, [3] dynamically tunes  $T$ , where it is named  $W$ , to adapt to the online monitored QoS. Therefore, a peak rate predictability analysis would provide an upper bound of  $T$ , and explore the CAC potential in gaining a maximized bandwidth utilization.

821 However, the above mentioned phenomenon  
822 reveals an “asymmetry” embedded in our pre-  
823 dictability definition, and shows its limitation in  
824 the peak rate case: Traffic valleys contribute more  
825 to the total prediction error than peaks. It is nat-  
826 ural since predictor tends to over-estimate the rate  
827 valley with a larger percentage than the rate peak.  
828 In mathematical words, given symmetric  $y_r (> \mu)$   
829 and  $y_l = 2\mu - y_r$  around the mean value, there are  
830 two corresponding components in  $P_{\text{err}}^Y(\tau, \varepsilon)$ : 830

$$P_{\text{err}}^{Y \geq y_r}(\tau, \varepsilon) = \Pr[\overline{\text{err}}(\tau) > \varepsilon, Y(t + \tau) \geq y_r]$$

$$= \int \int_{D1} f(x, y) dx dy,$$

$$P_{\text{err}}^{Y \leq y_l}(\tau, \varepsilon) = \Pr[\overline{\text{err}}(\tau) > \varepsilon, Y(t + \tau) \leq y_l]$$

$$= \int \int_{D2} f(x, y) dx dy,$$

831 where  $f(x, y)$  is the bivariate p.d.f. of the two in-  
832 dependent Gaussian variables ( $x$  and  $y$ ) in Fig. 11. 833  
834 The shadowed areas ( $D1$  and  $D2$ ) in the figure are  
835 circled by the following three lines:

$$L1: y = \frac{(y_r - \mu - \sqrt{\hat{\sigma}_\tau^2} x)}{\sqrt{\sigma^2 - \hat{\sigma}_\tau^2}};$$

$$L2: y = \frac{(y_l - \mu - \sqrt{\hat{\sigma}_\tau^2} x)}{\sqrt{\sigma^2 - \hat{\sigma}_\tau^2}};$$

$$L3: y = \frac{(-\varepsilon\mu - \sqrt{\hat{\sigma}_\tau^2} x)}{\varepsilon\sqrt{\sigma^2 - \hat{\sigma}_\tau^2}}.$$

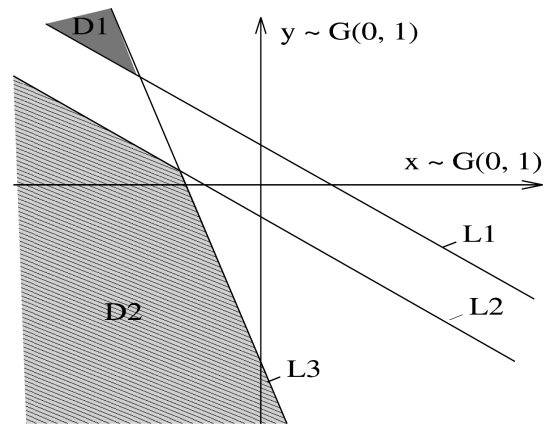


Fig. 11. Asymmetry in  $P_{\text{err}}^Y(\tau, \varepsilon)$ :  $P_{\text{err}}^{Y \geq y_r}(\tau, \varepsilon)$  ( $D1$ ) is smaller than  $P_{\text{err}}^{Y \leq y_l}(\tau, \varepsilon)$  ( $D2$ ) despite of  $(y_l + y_r)/2 = \mu$ .

837 Of the two components, the former is smaller  
 838 than the latter albeit  $y_l$  and  $y_s$  are symmetrically  
 839 located around  $\mu$ . This implies more bandwidth  
 840 over-subscription occurrence when  $Y(t + \tau)$   
 841 reaches its valley than peak. Therefore, we realize  
 842 that our predictability definition, by estimating the  
 843 mean BOSPr over the whole value range of  
 844  $Y(t + \tau)$ , may provide a deviated MPI estimation if  
 845 only traffic peak rate is the prediction target. In  
 846 dynamic bandwidth allocation that has a smaller  
 847 control time-scale, the definition works well since  
 848 the leftover bandwidth due to the bandwidth over-  
 849 subscription at this moment might absorb the  
 850 queued traffic load due to the under-subscription  
 851 at the last moment. Consequently the two parts in  
 852  $P_{\text{err}}(\tau, \varepsilon)$  offset each other, reflecting a balanced  
 853 predictability analysis. However, in CAC whose  
 854 control time-scale might be at buffer non-effective  
 855 region [14], the asymmetry would deteriorate  
 856 control performance with alternate in- and out-  
 857 profile service oscillation. In this scenario, another  
 858 definition of BOSPr is comparatively more rea-  
 859 sonable:

$$P_{\text{err}}(\tau, \varepsilon) \equiv \Pr[\overline{\text{err}}(\tau) > \varepsilon | Y(t + \tau) \geq y_r] \\ = \frac{\int_{D_1} f(x, y) dx dy}{1 - \Phi\left(\frac{y_r - \mu}{\sigma}\right)},$$

861 where  $\Phi(\circ)$  denotes the CDF of  $N(0, 1)$ , and  $y_r$  is  
 862 given as a ‘‘peak threshold’’ to describe the rate  
 863 region for traffic prediction. Then predictability  
 864 analysis can be done by applying such a BOSPr in  
 865 (1).

866 Different control situation may produce differ-  
 867 ent prediction constraint such as a small band-  
 868 width under-subscription percentage (BUSP) for  
 869 peak rate prediction, or small BUSP and BOSP at  
 870 the same time. As a result, traffic prediction should  
 871 consider the specific requirements from network  
 872 controller. This argument is illustrated in Fig. 12.  
 873 The dash lines there imply that the  $(P_\varepsilon, \varepsilon, \text{MPI})$ , as  
 874 the target of prediction performance metrics,  
 875 should be specified with reference to the control  
 876 parameters. Each vertex of the solid-line triangle  
 877 denotes a metrics measure and its target. Any two  
 878 vertices can unite together to decide the third one  
 879 for given traffic process. This diagram outlines our

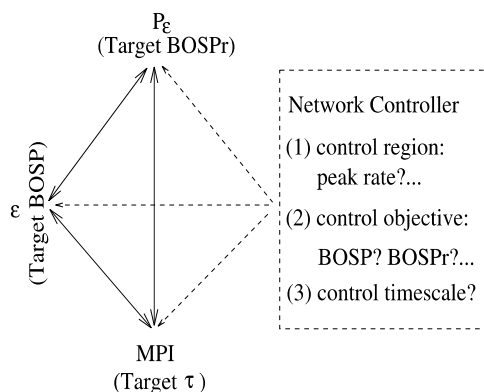


Fig. 12. Guideline to prediction analysis: to evaluate (BOSP, BOSPr,  $\tau$ ) using  $(P_\varepsilon, \varepsilon, \text{MPI})$  as expected by controller.

880 way to view traffic prediction and to do predict-  
 881 ability analysis.

882 Actually the above argument is not limited to  
 883 ARMA prediction. For MMPP, the unsymmetric  
 884 phenomenon is shown by the non-monotonic  
 885  $P_{\text{err}_i}(\tau, \varepsilon)$  being a function of  $\tau$ , as found in our  
 886 simulation. Under this circumstance, predictability  
 887 analysis should be adjusted similarly. For example,  
 888 if we intend to predict peak rate process defined by  
 889 a peak threshold  $r_i$  and a given  $P_\varepsilon$ , a changed index  
 890 set  $\{i\}^* = \{i | r_i \geq r_i\}$  should replace the original  $\{i\}$   
 891 set in (13), so that BOSPr becomes:  
 892  $P_{\text{err}_i}(\tau, \varepsilon) = \sum_{\{i\}^*} P_{\text{err}_i}(\tau, \varepsilon) / |\{i\}^*|$ . With this change,  
 893 other analysis can proceed in the same way.

894 Previously we discussed the ARMA and MMPP  
 895 modeling validity in case of self-similar traffic of  
 896 LRD. We believe that for the limited control time-  
 897 scales in a realistic ATM network of tight QoS  
 898 constraint, the models derive good approximation.  
 899 Searching for the best prediction model is beyond  
 900 our purpose. On the one hand, LRD property may  
 901 improve the non-trivial short-term prediction, if  
 902 viewed with 2nd-order property only. On the other  
 903 hand, LRD traffic can still be very bursty (thus  
 904 hard to predict), if evaluated by variance coeffi-  
 905 cient. To make things more complicated, real  
 906 traffics can be highly non-stationary and of both  
 907 SRD and LRD components at multiple time-  
 908 scales. Self-similar models of two to three param-  
 909 eters only, though claimed to capture all-scale  
 910 traffic granularity, need cautious study for online  
 911 prediction under strict error constraint. With the

912 consideration of the 1st-order statistics (e.g. a  
913 long-tail distribution like Pareto), the prediction-  
914 based control efficiency and the limited time-scales  
915 requirements, self-similar traffic predictability with  
916 other models deserves further research. However,  
917 both the Gaussian confidence interval and the  
918 mean rate estimation in the analysis need to be re-  
919 considered.

## 920 6. Conclusion

921 This paper investigates network traffic predict-  
922 ability in order to explore the potential or optimal  
923 bounds of multi-step traffic prediction in traffic  
924 engineering. We are especially interested in deriv-  
925 ing the upper/lower values of prediction interval or  
926 error for representative traffic traces collected from  
927 real networks. Having the bound solution is  
928 equivalent to achieving the optimal prediction of  
929 each given traffic trace. Then it can be used to  
930 estimate specific control performance, or select  
931 certain control parameters such as the control  
932 time-scale or bandwidth utilization target. Our  
933 analysis is based on two popular models—ARMA  
934 and MMPP—for their available optimal predic-  
935 tors and their popularity in practice.

936 We believe that the tradeoff between a large  
937 MPI and a small prediction error reveals the  
938 tradeoff between a selected control time-scale and  
939 the corresponding control efficiency. Furthermore,  
940 the paper shows that proper traffic measurement  
941 (i.e. low-pass filtering) and multiplexing (i.e. ag-  
942 gregating) improves predictability. Both the 1st-  
943 and 2nd-order traffic statistics matters in the  
944 analysis. Moreover, particular traffic properties  
945 like multiple correlation time-scales, large variance  
946 coefficient and SRD limit prediction performance.  
947 Extensive numerical studies of real traces verify  
948 these analytical observations. More specifically,  
949 this derives the insights in favor of aggregated, in  
950 contrast to per-flow, traffic prediction at limited  
951 time-scales. Through an engineering-oriented off-  
952 line study given complete traffic knowledge, we  
953 would be able to evaluate the online prediction  
954 gain and loss, and to estimate the prediction-based  
955 control efficiency in practice.

## References

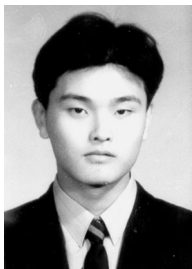
- 957  
958  
959  
960  
961  
962  
963  
964  
965  
966  
967  
968  
969  
970  
971  
972  
973  
974  
975  
976  
977  
978  
979  
980  
981  
982  
983  
984  
985  
986  
987  
988  
989  
990  
991  
992  
993  
994  
995  
996  
997  
998  
999  
1000  
1001  
1002  
1003  
1004  
1005  
1006  
1007  
1008  
1009  
1010  
1011
- [1] A. Adas, Using adaptive linear prediction to support real-time VBR video under RCBP network service model, *IEEE/ACM Trans. Network* 6 (5) (1998) 635–644.
  - [2] The Internet Traffic Archive, Bellcore Ethernet Traces, <http://www.acm.org/sigcomm/ITA>.
  - [3] C. Casetti, J. Kurose, D. Towsley, An adaptive algorithm for measurement-based admission control in integrated services packet networks, *International Workshop on Protocols for High Speed Networks*, Sophia Antipolis, 1996.
  - [4] R.L. Easton, P.T. Hutchinson, R.W. Moncello, R.W. Muise, TASI-E communications system, *IEEE Trans. Commun.* (1982) 803–807.
  - [5] Insight into current Internet traffic workloads, Fix-West NAP Trace, <http://www.nlanr.net/NA>.
  - [6] M.W. Garrett, W. Willinger, Analysis, modeling and generation of self-similar VBR video traffic, in: *SIGCOMM'94*, 1994, pp. 268–280, The JPEG traces can be downloaded from <ftp://thumper.bellcore.com/pub/vbr.video.trace>.
  - [7] M. Grossglauser, D. Tse, A framework for robust measurement-based admission control, *IEEE/ACM Trans. Network* 7 (3) (1999) 293–309.
  - [8] S. Haykin, L. Li, Nonlinear adaptive prediction of nonstationary signals, *IEEE Trans. Signal. Process.* 43 (2) (1995) 526–535.
  - [9] S. Jamin, P.B. Danzig, S.J. Shenker, L. Zhang, A measurement-based admission control algorithm for integrated services packet network, *SIGCOMM'95*, Cambridge, MA, USA, 1995.
  - [10] S.K. Mitra, J.F. Kaiser (Eds.), *Handbook for Digital Signal Processing*, Wiley & Sons, New York, 1993.
  - [11] M.B. Priestley, *Spectral Analysis and Time Series*, Academic Press, New York, 1992.
  - [12] O. Rose, Statistical properties of MPEG video traffic and their impact on traffic modeling in ATM systems, *Technical Report 101*, Institute of Computer Science, University of Wurzburg, 1995. The MPEG-1 traces can be downloaded from <ftp://thumper.bellcore.com/pub/vbr.video.trace>.
  - [13] S. Chong, S.Q. Li, J. Ghosh, Predictive dynamic bandwidth allocation for efficient transport of real-time VBR video over ATM, *IEEE. JSAC.* 13 (1) (1995) 12–23.
  - [14] Y. Kim, S.Q. Li, Time-scale of interest in traffic management for link bandwidth allocation design, *Proc. IEEE Infocom'96 Conference*, 1996, pp. 738–748.
  - [15] J. Ye, S.Q. Li, Folding algorithm: a computational method for finite QBD processes with level-dependent transitions, *IEEE Trans. Commun.* 42 (2) (1994) 625–639.
  - [16] S.Q. Li, C. Hwang, Queue response to input correlation functions: continuous spectral analysis, *IEEE/ACM. Trans. Network* 1 (6) (1993) 678–692.
  - [17] S.Q. Li, C. Hwang, On the convergence of traffic measurement and queueing analysis: a statistical-match and queueing (SMAQ) tool, *IEEE/ACM Trans. Network.* (April) (1997) 95–110.



- 1012  
1013  
1014  
1015  
1016  
1017  
1018  
1019  
1020  
1021  
1022  
1023  
1024  
1025  
1026  
1027  
1028  
1029  
1030  
1031  
1032  
1033  
1034  
1035  
1036  
1037  
1038  
1039  
1040  
1041  
1042  
1043  
1044  
1045
- [18] J.D. Pruneski, S.Q. Li, The linearity of low frequency traffic flow: an intrinsic I/O property in queueing systems, Proc. IEEE Infocom'95 Conference, April 1995, pp. 613-623, also to appear in IEEE/ACM Trans. Network.
- [19] I. Norros, On the use of fractional Brownian motion in the theory of connectionless networks, IEEE JSAC 13 (6) (1997) 953-962.
- [20] T. Tuan, K. Park, Multiple time scale congestion control for self-similar network traffic, Perform. Evaluation, in press.
- [21] W. Leland, M. Taqqu, W. Willinger, D. Wilson, On the self-similar nature of Ethernet traffic (extended version), IEEE Trans. Network 2 (1) (1994).
- [22] J. Beran, R. Sherman, M. Taqqu, W. Willinger, Long-range dependence in variable-bit-rate video traffic, IEEE Trans. Network 43 (2/3/4) (1995).
- [23] M. Garrett, W. Willinger, Analysis, modeling and generation of self-similar VBR video traffic, SIGCOMM, 1994.
- [24] M. Crovella, A. Bestavros, Self-similarity in World Wide Web traffic: evidence and possible causes, IEEE Trans. Network 5 (6) (1997).
- [25] D. Heyman, T. Lakshman, What are the implication of long-range dependence for VBR-video traffic engineering, IEEE Trans. Network 4 (3) (1996).
- [26] B. Ryu, A. Elwalid, The importance of long-range dependence of VBR video traffic in ATM traffic engineering: myths and realities, ACM Comput. Commun. Rev. 26 (1996) 3-14.
- [27] N. Likhanov, R. Mazumdar, Cell loss asymptotics in buffers fed with a large number of independent stationary sources, IEEE INFOCOM Proceedings, 1998.
- [28] M. Montgomery, G. de Veciana, On the relevance of time scales in performance oriented traffic characterizations, IEEE INFOCOM Proceedings, San Francisco, CA, 1996.



**San-qi Li** received his B.S. degree from Beijing University of Posts and Telecommunications, Beijing, China, in 1976, and the M.A.Sc. and Ph.D. degree from the University of Waterloo, Waterloo, ON, Canada, in 1982 and 1985, respectively, all in Electrical Engineering. From 1985 to 1989, he was Associate Research Scientist and Principal Investigator at Center for Telecommunications Research at Columbia University, New York in September 1989, he joined the faculty of the Department of Electrical and Computer Engineering, The University of Texas at Austin, where he is Temple Foundation Endowed Professor. He is also an Honorable Professor at Beijing University of Posts and Telecommunication, China. He has published more than 150 papers in international archival journals and referred international conference proceedings. The main focus of his research has been to develop new analytical methodologies and carry out performance analysis of multimedia service networks, then understand system fundamentals and explore new design concepts. Dr. Li served as a Member of the Technical Program Committee for IEEE Infocom Conference since 1988 to 1998. From 1995 to 1997, he served as an Editor for IEEE/ACM Transaction on Networking.



**Aimin Sang** was born in Shandong Province, China in 1974. He received his Ph.D. from the Department of Electrical and Computer Engineering, the University of Texas at Austin in May, 2001. His dissertation was focused on measurement-based traffic management for QoS guarantee in multi-service networks, under the supervision of Prof. San-qi Li. He received his M.S. (1996) from Institute of Automation, Chinese Academy of Sciences, under the supervision of Prof. Ru-Wei Dai, President of Chinese Association of Automation. He earned his B.S. (1993) from University of Science and Technology of China (USTC) in Electrical Engineering. He joined Santera System Inc. in May, 2000, where he is now a member of technical staff and firmware engineer and is involved in developing the next-generation multi-service switch (Media Gateway+Media Gateway Controller+Signaling Gateway). He designed and implemented measurement-based CAC algorithm for the SanteraOne system, and finished a series of ATM projects. His research interests include scalable DiffServ in a MPLS network, cooperative web caching, re-routing and stability issue in (optical) networks, and fundamental issues in measurement-based network resource management.